Antisite defects and traps in perovskite $YAlO_3$ and $LuAlO_3$: Density functional calculations

D. J. Singh
Materials Science and Technology Division and Center for Radiation Detection Materials and Systems, Oak Ridge National Laboratory, Oak Ridge, Tennessee 37831-6114, USA
(Received 1 September 2007; published 26 December 2007)

Density functional calculations in supercells are used to investigate antisite point defects in $YAlO_3$ and $LuAlO_3$. It is found that antisites consisting of an Al on the Y(Lu) site and those consisting of an Y(Lu) on the Al site both have low energy with respect to binary oxide reservoirs. Defects containing Al on the *A* site yield electron traps at 0.4–0.8 eV below the conduction band edge, while Y(Lu) ions on the Al site do not. Based on this it is suggested that growth conditions that avoid Al on the *A* site may reduce the number of electron traps in these materials.

DOI: 10.1103/PhysRevB.76.214115 PACS number(s): 61.72.Bb, 71.20.Ps, 71.55.Ht

I. INTRODUCTION

Perovskite $YAlO_3$ and $LuAlO_3$ are of interest as laser hosts[1,2] and when activated with Ce^{3+} as scintillators for radiation detection.[3–13] Two key factors that control the performance of scintillators in spectroscopic radiation detection are light yield, i.e., the number of photons per unit of energy deposited, and proportionality, which measures the linearity of the light output with γ-ray energy.[14–20] These perovskites have good light yields and $YAlO_3$ activated with Ce^{3+}, in particular, is remarkable in its extremely proportional response.[12,16] Recently, there has been a focus on carrier traps, for which evidence is found in thermoluminescence experiments, as a limiting factor for the performance of these perovskite aluminates.[10,21–27]

Atomistic simulations[25–27] using empirical potentials found that the antisite defect in which an Al and *A*-site (Y,Lu) atom are interchanged had a lower energy than Schottky or Frenkel defects. Based on these results this antisite defect was associated with the trap states seen in thermoluminescence that degrade the scintillator performance of these materials. The purpose of this paper is to extend those results using first principles electronic structure calculations and to investigate other antisite point defects, specifically isolated Al on the Y(Lu) site and isolated Y(Lu) on the Al site.

II. APPROACH

The calculations reported here were done using the general potential linearized augmented plane wave (LAPW) method including local orbitals.[28,29] LAPW sphere radii of $1.5a_0$, $1.8a_0$, $2.05a_0$, and $2.05a_0$ were used for O, Al, Y, and Lu, respectively. Tests were done using other choices of sphere radii and the results were found to be stable. Well converged basis sets were employed, using local orbitals and plane wave cutoff k_{max} given by $R_O k_{max}=7.0$, where R_O is the oxygen sphere radius. This yields effective values of Rk_{max} of 8.4 for Al and 9.56 for Y and Lu. The defect energies were calculated using 40-atom supercells (constructed by a $\sqrt{2}\times 1\times\sqrt{2}$ doubling of the 20-atom *Pnma* cell). The lattice parameters were taken from experiment but all internal atomic positions were fully relaxed and no symmetry constraints were imposed. We focus on the case where the compounds are fully oxidized and use Al_2O_3, Y_2O_3, and Lu_2O_3 as reference systems.

The structure of corundum (Al_2O_3) has been well established by many experimental studies.[30,31] Here, we used the experimental structure from neutron diffraction of Toebbens *et al.*[31] The calculated forces on the atoms were small, the largest being $0.005\ \mathrm{Ry}/a_0$. Similarly, for Y_2O_3 we found only small forces ($<0.005\ \mathrm{Ry}/a_0$) with the experimental crystal structure.[32] For the other materials studied, we used the experimental lattice parameters as determined by diffraction, but relaxed the internal coordinates. The structures used are summarized in Tables I and II. The relaxed local-density approximation (LDA) structures are similar to experimental data, where available,[32–35] and in the case of Lu_2O_3 to previous density functional results.[36,37]

III. ENERGETICS

The calculated enthalpies of formation of the perovskite phase from corundum Al_2O_3 and cubic Y_2O_3 were determined by subtraction of the relevant total energies for the reaction

$$\tfrac{1}{2}Al_2O_3 + \tfrac{1}{2}Y_2O_3 \rightarrow YAlO_3 \qquad (1)$$

and similarly for $LuAlO_3$. The LDA enthalpies of formation are exothermic, as expected, and are −22 and −34 kJ/mol,

TABLE I. Structural parameters of cubic Lu_2O_3 space group $Ia\bar{3}$, lattice parameters from experimental diffraction $a=10.391$ Å, and $a=10.5981$, for Lu_2O_3 and Y_2O_3, respectively. The internal coordinates, Lu1 (1/4,1/4,1/4), Lu2 (x,0,1/4), and O (x,y,z), are by total energy minimization, while those of Y_2O_3 are the experimental data of Ref. 32. There are eight formula units per primitive cell.

	Lu_2O_3 (LDA)	Y_2O_3 (Expt.)
Lu2 x	0.9666	0.96764
O x	0.3908	0.3907
O y	0.1517	0.1518
O z	0.3800	0.3801

TABLE II. Structural parameters of Lu_2O_3 and Y_2O_3. Space group *Pnma* and lattice parameters from experimental diffraction $a=5.334\ 17$ Å, $b=7.305\ 32$ Å, and $c=5.105\ 64$ Å for $LuAlO_3$ (Ref. 33), and $a=5.330$ Å, $b=7.375$ Å, and $c=5.180$ Å for $YAlO_3$ (Ref. 34). The internal coordinates, Y(Lu) $(x,1/4,z)$, Al $(0,0,1/2)$ O1 $(x,1/4,z)$, O2 (x,y,z), are by total energy minimization and compared with x-ray refinement (expt.). There are four formula units per primitive cell.

	$LuAlO_3$	$LuAlO_3$ (Expt.)	$YAlO_3$	$YAlO_3$ (Expt.)
Lu/Y x	0.0659	0.0632	0.0562	0.0526
Lu/Y z	0.9824	0.9832	0.9868	0.9896
O1 x	0.4685	0.482	0.4756	0.475
O1 z	0.1021	0.088	0.0884	0.086
O2 x	0.2999	0.291	0.2949	0.293
O2 y	0.0528	0.054	0.0465	0.044
O2 z	0.6986	0.698	0.7045	0.703

for $LuAlO_3$ and $YAlO_3$, respectively. The perovskite geometric tolerance factors $t=(r_A+r_O)/\sqrt{2}(r_{Al}+r_O)$, where r_A, r_{Al}, and r_O are the *A*-site, Al, and O ionic radii[38] of $LuAlO_3$ and $YAlO_3$, are 0.89 and 0.91, respectively, consistent with the *Pnma* $GdFeO_3$ structures observed. Thus, these energies follow the trend of reduced perovskite stability at low tolerance factor. We note that in general the combination of low tolerance factor and similar *A*- and *B*-site charge, which occurs in $LuAlO_3$ and $YAlO_3$, may be expected to be favorable for cation antisite defects in perovskites.

The enthalpies of formation of the perovskites from the binary oxides as above were also calculated using the generalized gradient approximation of Perdew, Burke, and Ernzerhof (PBE).[39] This was done using the WIEN2K code.[40] The use of the PBE functional lowered the stability relative to the LDA of the perovskite phase by ~10 kJ/mol for $LuAlO_3$ and by ~20 kJ/mol for $YAlO_3$. If these differences are indicative of the LDA errors, they would be of importance for predicting the formation conditions of the perovskite but of less significance compared to the large energies of the defects calculated below.

Turning to the supercell calculations, we obtained the energy of the antisite defect by comparing the total energy of a perfect cell with that of cells with single Y(Lu)-Al interchanges and relaxation of the atomic positions. Again we find the expected trend with ionic size, that is, that the energy for the antisite is lower in $LuAlO_3$, which has a lower tolerance factor, corresponding to smaller difference between the *A*-site and Al radii. The calculated energies are, however, significantly larger than those obtained previously using empirical potentials. We obtain the antisite defect formation energies as 3.4 eV in $LuAlO_3$ and 4.4 eV in $YAlO_3$ (320 and 430 kJ/mol, respectively). While these are not so high as to completely preclude the existence of these defects in the materials, they are significantly higher than the values obtained previously with empirical potentials (2.7 and 3.1 eV, respectively).[27,41] We note that in scintillator applications Ce^{3+} concentrations at the 0.1% level are typically used for activation and that strong effects of traps are not expected for trap concentrations that are extremely small compared to the concentration of activator sites.

TABLE III. Calculated LDA defect energies of *Pnma* $LuAlO_3$ and $YAlO_3$ based on 40-atom supercells including relaxation of the atomic positions. The notation is that A_B denotes an atom of type *A* on a site of composition *B* in the perfect crystal, and A_BB_A denotes the antisite, which here is interchange of neighboring *A* and *B* atoms (sometimes called the antisite pair).

	$YAlO_3$ (eV)	$LuAlO_3$ (eV)
$Al_{Y(Lu)}$	2.5	2.1
$Y(Lu)_{Al}$	2.4	1.6
$Al_{Y(Lu)}Y(Lu)_{Al}$	4.4	3.4

In order to proceed, we considered the energies of an Al on an *A* site, relative to reservoirs of Al_2O_3 and $Y(Lu)_2O_3$, and also the energies of Lu(Y) on the Al site with the same reservoirs. For example, we calculated the energy of the defect consisting of an Y on an Al site via the formula

$$\tfrac{1}{2}Y_2O_3 + nYAlO_3 \rightarrow \tfrac{1}{2}Al_2O_3 + nYAlO_3 + Y_{Al}, \qquad (2)$$

where Y_{Al} denotes the defect and $n=8$ for the supercells that were used.

The calculated energies are summarized in Table III. As expected, the sums of the half-anti-site energies are larger than the antisite energy, reflecting an attractive interaction between these half-anti-sites, which is normally present due to strain. The attractive energy is 0.35 eV in $LuAlO_3$ and 0.53 eV in $YAlO_3$, again following the expected trend with tolerance factor (greater strain when the difference in *A*-site and *B*-site radii is larger). In any case, these energies are much lower than the stoichiometric antisite, and therefore these defects should be much more prevalent. The relative concentrations of these defects will depend on the chemical environment during synthesis (yttria and/or lutetia rich vs alumina rich).

IV. ELECTRONIC STRUCTURES

The band structures of $YAlO_3$ and $LuAlO_3$ for the orthorhombic structure are shown in Fig. 1. As noted previously,[42,43] the gaps are subject to the usual underestimation in LDA calculations. The calculated LDA band gaps are 5.8 and 5.6 eV for $LuAlO_3$ and $YAlO_3$, respectively. The experimental gaps are above 8.4–8.8 eV.[44] We find similar underestimates for the band gaps of the binary oxides. The calculated LDA gaps are 3.4, 4.0, and 6.2 eV for Lu_2O_3, Y_2O_3, and Al_2O_3, respectively, as compared with experimental values[45] of ~6 eV for Y_2O_3 and Lu_2O_3 and ~9 eV for Al_2O_3.[46] As expected, the valence bands of the perovskites are derived from O *p* states, while the conduction bands have free electron character derived from Al and Y(Lu) states as well as Y(Lu) *d* character.

The electronic structures (Fig. 2) for the supercells with the antisite defect in which an Al and an Y/Lu *A*-site ion are interchanged do, in fact, show a split-off state below the conduction band edge. This state, as characterized by the LDA eigenvalue, is 0.5 eV below the conduction band edge for $YAlO_3$ and 0.8 eV below for $LuAlO_3$. Thus from this

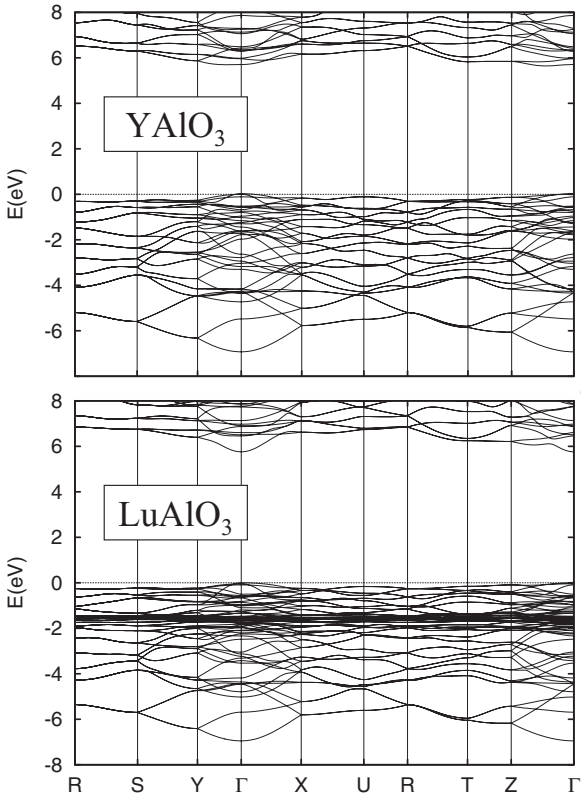

FIG. 1. LDA band structure of orthorhombic $YAlO_3$ (top) and $LuAlO_3$ (bottom). The dense set of bands at ~−1.5 eV in $LuAlO_3$ are the Lu $4f$ states.

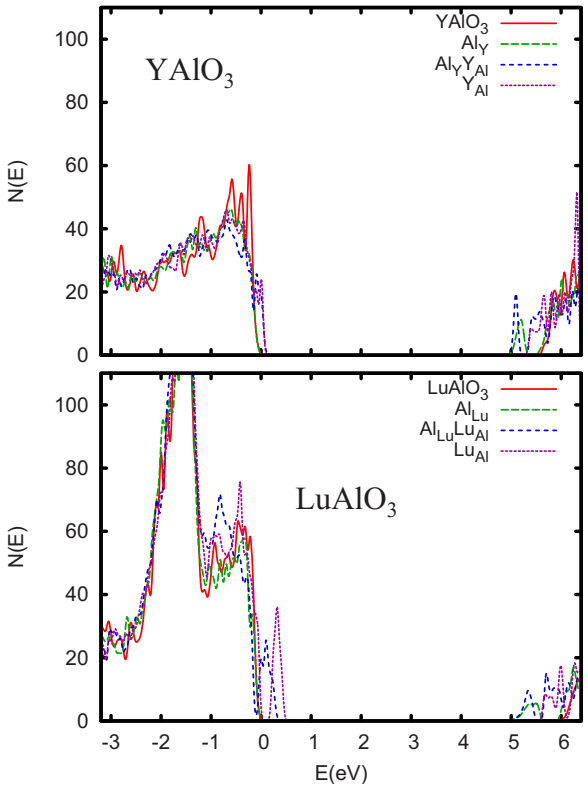

FIG. 2. (Color online) LDA densities of states of 40-atom supercells of $YAlO_3$ (top) and $LuAlO_3$ with and without defects. The notation is as in Table III. The density of states was obtained using 52 **k** points in the Brillouin zone and a Gaussian broadening of width 0.04 eV.

point of view, the stoichiometric antisite could explain the electron traps seen in these materials as suggested previously.[27] Such a state is not seen in the supercells with an Y(Lu) on the Al site.[47] However, the supercells with an Al on the A site do show a trap state, in this case 0.4 eV below the conduction band minimum for $YAlO_3$ and 0.7 eV below for $LuAlO_3$.

We note that there may be some errors in the trap energies as characterized by LDA eigenvalues due to LDA band gap underestimation and other correlation effects. Nonetheless, because these are deep levels formed from conduction band states in a wide band gap material, they are expected to persist as the band gap is corrected. This is because the LDA usually provides a good description of the chemical bonding in this type of material, and removal of the trap would mean a change in ionic character and bonding of the system with an electron. It should also be noted that there are states pulled to the bottom of the conduction band by Lu(Y) on an Al site. These do not separate from the conduction band, but it is possible that they may do so in larger supercells, to yield more shallow traps. Also, for both compounds with defects where a A-site, Y(Lu) ion occurs on the B-site, the valence band edge is broadened, and in the case of $LuAlO_3$ with a Lu on the B site, a shallow density of states peak appears in the gap at ~0.3 eV above the valence band edge. This peak contains three states of Lu $f-O$ p antibonding character. These are associated with the Lu atom on the Al site. Without correlation effects the presence of such states would indicate a hole trap. However, this may not be the case because of the f character of the state which would make correlation effects (especially self-interaction) important.

Because the formation energy for an Al on the A site is much lower than that for the Al-Y(Lu) interchange, this type of defect is a more likely source of the traps in $YAlO_3$ and $LuAlO_3$ crystals. The origin of the trap states can be understood simply in terms of crystal chemistry. Specifically, in oxides extended free electron conduction states are pushed up in energy relative to more localized states (d states) because of the limited volume available in the crystalline environment. When a small Al ion is placed on the large A site, this mechanism is less effective. This brings the states associated with the Al on the A site down in energy thus leading to trap states in the gap.

V. SUMMARY AND CONCLUSIONS

To summarize, supercell calculations for perovskite $LuAlO_3$ and $YAlO_3$ show that single antisites in which an Al is placed on the Y(Lu) site or an Y(Lu) atom is placed on the Al site are low energy defects with respect to reservoirs of the binary oxides. Y(Lu) atoms on the Al site do not produce strong electron traps in the gap. However, defects containing Al atoms on the Y(Lu) sites do produce traps at 0.4–0.8 eV below the conduction band edges. Since the energies of both types of single antisite are low, these types of defects prob-

ably cannot be entirely eliminated in conventional crystal growth methods. However, since only one type (Al on *A* site) produces an electron trap, it may be possible to reduce the number of trap states by controlling the growth conditions, particularly by going to Y(Lu) rich conditions, provided that binary inclusions and other defects that produce traps such as vacancies can be avoided.

ACKNOWLEDGMENTS

We are grateful for helpful discussions with M. H. Du, L. A. Boatner, G. E. Jellison, Jr., and J. S. Neal. This work was supported by the Department of Energy, Office of Nonproliferation Research and Development, NA22.

[1] M. J. Weber, M. Bass, K. Andringa, R. R. Monchanp, and E. Comperchio, Appl. Phys. Lett. **15**, 342 (1969).
[2] G. A. Massey, Appl. Phys. Lett. **17**, 213 (1970).
[3] M. J. Weber, J. Appl. Phys. **44**, 3205 (1973).
[4] T. Takeda, T. Miyata, F. Muramatsu, and T. Tomiki, J. Electrochem. Soc. **127**, 438 (1980).
[5] V. G. Baryshevsky, M. V. Korzhik, B. I. Minkov, S. A. Smimova, A. A. Fyodorov, P. Dorenbos, and C. W. E. van Eijk, J. Phys.: Condens. Matter **5**, 7893 (1993).
[6] A. Lempicki, M. H. Randles, D. Wisniewski, M. Balcerzyk, C. Brecher, and A. J. Wojtowicz, IEEE Trans. Nucl. Sci. **NS-42**, 280 (1995).
[7] S. Baccaro, K. Blacek, F. de Notaristefani, P. Maly, J. A. Mares, R. Pani, R. Pellegrini, and A. Soluri, Nucl. Instrum. Methods Phys. Res. A **361**, 209 (1995).
[8] K. S. Shah, P. Bennett, and M. R. Squillante, IEEE Trans. Nucl. Sci. **NS-43**, 1267 (1996).
[9] M. Moszynski, D. Wolski, T. Ludziejewski, M. Kapusta, A. Lempicki, C. Brecher, D. Wisniewski, and A. J. Wojtowicz, Nucl. Instrum. Methods Phys. Res. A **385**, 123 (1997).
[10] W. Drozdowski, D. Wisiewski, A. J. Wojtowicz, A. Lempicki, P. Derenbos, J. T. M. de Haas, C. W. E. van Eijk, and A. J. J. Bos, J. Lumin. **72-74**, 756 (1997).
[11] A. J. Wojtowicz, J. Glodo, W. Drozdowski, and K. R. Przegietka, J. Lumin. **79**, 275 (1998).
[12] M. Kapusta, M. Balcerzyk, M. Moszynski, and J. Pawelke, Nucl. Instrum. Methods Phys. Res. A **421**, 610 (1999).
[13] P. Szupryczynski, M. A. Spurrier, C. J. Rawn, C. L. Melcher, and A. A. Carey, IEEE Nucl. Sci. Symp. Conf. Rec. **3**, 1305 (2005).
[14] P. Dorenbos, J. T. M. de Haas, and C. W. E. van Eijk, IEEE Trans. Nucl. Sci. **NS-42**, 2190 (1995).
[15] B. D. Rooney and J. D. Valentine, IEEE Trans. Nucl. Sci. **NS-43**, 1271 (1996).
[16] W. Mengesha, T. D. Taulbee, B. D. Rooney, and J. D. Valentine, IEEE Trans. Nucl. Sci. **NS-45**, 456 (1998).
[17] M. Balcerzyk, M. Moszynski, M. Kapusta, D. Wolski, J. Pawelke, and C. L. Melcher, IEEE Trans. Nucl. Sci. **NS-47**, 1319 (2000).
[18] W. W. Moses, Nucl. Instrum. Methods Phys. Res. A **487**, 123 (2002).
[19] M. Moszynski, Nucl. Instrum. Methods Phys. Res. A **505**, 101 (2003).
[20] J. E. Jaffe, D. V. Jordan, and A. J. Peurrung, Nucl. Instrum. Methods Phys. Res. A **570**, 72 (2007).
[21] A. Vedda, M. Martini, F. Meinardi, J. Chval, M. Dusek, J. A. Mares, E. Mihokova, and M. Nikl, Phys. Rev. B **61**, 8081 (2000).
[22] A. J. Wojtowicz, P. Szuprysczynski, D. Wisniewski, J. Glodo, and W. Drozdowski, J. Phys.: Condens. Matter **13**, 9599 (2001).
[23] M. Nikl, J. A. Mares, J. Chval, E. Mihokova, N. Solovieva, M. Martini, A. Vedda, K. Blazek, P. Maly, K. Nejezchleb, P. Fabeni, G. P. Pazzi, V. Babin, K. Kalder, A. Krasnikov, S. Zazubovich, and C. D'Ambrosio, Nucl. Instrum. Methods Phys. Res. A **486**, 250 (2002).
[24] M. Nikl, V. V. Laguta, and A. Vedda, Phys. Status Solidi A **204**, 683 (2007).
[25] M. M. Kuklja, J. Phys.: Condens. Matter **12**, 2953 (2000).
[26] C. R. Stanek, M. R. Levy, K. J. McClellan, B. P. Uberuaga, and R. W. Grimes, Phys. Status Solidi B **242**, R113 (2005).
[27] C. R. Stanek, K. J. McClellan, M. R. Levy, and R. W. Grimes, J. Appl. Phys. **99**, 113518 (2006).
[28] D. J. Singh and L. Nordstrom, *Planewaves, Pseudopotentials and the LAPW Method*, 2nd ed (Springer, Berlin, 2006).
[29] D. Singh, Phys. Rev. B **43**, 6388 (1991).
[30] S. Pillet, M. Souhassou, C. Lecomte, K. Schwarz, P. Blaha, M. Rerat, A. Lichanot, and P. Roversi, Acta Crystallogr., Sect. A: Found. Crystallogr. **57**, 290 (2001).
[31] D. M. Toebbens, N. Stuesser, K. Knorr, H. M. Mayer, and G. Lampert, Mater. Sci. Forum **378**, 288 (2001).
[32] E. N. Maslen, V. A. Streltsov, and N. Ishizawa, Acta Crystallogr., Sect. B: Struct. Sci. **52**, 414 (1996).
[33] L. Vasylechko, D. M. Trots, A. Senyshyn, and T. Lukasiewicz, HASYLAB 2006 Annual Report, 2006 (unpublished), p. 605.
[34] R. Diehl and G. Brandt, Mater. Res. Bull. **10**, 85 (1975).
[35] N. L. Ross, J. Zhao, and R. J. Angel, J. Solid State Chem. **177**, 1276 (2004).
[36] N. Hirosaki, S. Ogata, and C. Kocer, J. Alloys Compd. **351**, 31 (2003).
[37] L. Marsella and V. Fiorentini, Phys. Rev. B **69**, 172103 (2004).
[38] R. D. Shannon, Acta Crystallogr., Sect. A: Cryst. Phys., Diffr., Theor. Gen. Crystallogr. **32**, 751 (1976).
[39] J. P. Perdew, K. Burke, and M. Ernzerhof, Phys. Rev. Lett. **77**, 3865 (1996).
[40] P. Blaha, K. Schwarz, G. K. H. Madsen, D. Kvasnicka, and J. Luitz, WIEN2K, an augmented plane wave plus local orbitals program for calculating crystal properties, Vienna University of Technology, Austria, 2001.
[41] The values were extracted from Fig. 1 of Ref. 27.
[42] D. M. Bercha, K. Z. Rushchanskii, M. Sznajder, A. Matkovskii, and P. Potera, Phys. Rev. B **66**, 195203 (2002).
[43] G. Pari, A. Mookerjee, and A. K. Bhattacharya, Physica B **353**, 192 (2004).
[44] V. Kolobanov, V. Mikhailin, N. Petrovnin, D. Spassky, and Y. Zorenko, Phys. Status Solidi B **243**, R60 (2006).
[45] G. Seguini, E. Bonera, S. Spiga, G. Scarel, and M. Fanciulli, Appl. Phys. Lett. **85**, 5316 (2004).
[46] M. L. Bortz and R. H. French, Appl. Phys. Lett. **55**, 1955 (1989).
[47] Due to the finite size of the supercell, we cannot exclude a shallow state near the band edge for Y(Lu) on the Al site.